REGULAR ARTICLE

Distinct Na$^+$/K$^+$/2Cl$^-$ cotransporter localization in kidneys and gills of two euryhaline species, rainbow trout and killifish

Fumi Katoh · Regina R. F. Cozzi · William S. Marshall · Greg G. Goss

Abstract The kidney is an organ playing an important role in ion regulation in both freshwater (FW) and seawater (SW) fish. The mechanisms of ion regulation in the fish kidney are less well studied than that of their gills, especially at the level of transporter proteins. We have found striking differences in the pattern of Na$^+$/K$^+$/2Cl$^-$ cotransporter (NKCC) expression between species. In the killifish kidney, NKCC is apically localized in the distal and collecting tubules and basolaterally localized in the proximal tubules. However, in the SW killifish gill, NKCC is basolaterally co-localized with Na$^+$/K$^+$-ATPase, whereas in FW, NKCC immunoreactivity is primarily apical, although still colocalized within the same mitochondria-rich cell with basolateral Na$^+$/K$^+$-ATPase. Rainbow trout kidney has NKCC only in the apical membrane of the distal and collecting tubules in both environments, with no signal being detected in the proximal tubule. On the other hand, in the trout gill, NKCC is found basolaterally in both FW and SW environments. An important observation is that, in the gills of rainbow trout, the trailing edge of the filament possesses mostly Na$^+$/K$^+$-ATPase-positive but NKCC-negative mitochondria-rich cells, whereas in the region between and at the roots of the gill lamellae, most mitochondria-rich cells exhibit both Na$^+$/K$^+$-ATPase- and NKCC-positive immunoreactivity. These results suggest that the differential localization of transporters between the two species represents differences in function between these two euryhaline fishes with different life histories and strategies.

Keywords Mitochondria-rich cells · Kidney · Gill · Na$^+$/K$^+$/2Cl$^-$ cotransporter · Killifish, *Fundulus heteroclitus* · Rainbow trout, *Oncorhynchus mykiss* (Teleostei)

Introduction

Teleosts maintain their ion concentration and osmolality of the body fluid within a narrow physiological range that is often different from the environmental ion levels. Two model organisms selected for this study are the killifish (*Fundulus heteroclitus*) and rainbow trout (*Oncorhynchus mykiss*) since they represent two of the most studied fish species for ion transport. Whereas the contribution of gills and branchial mitochondria-rich cells to ion regulation has been extensively studied in both species (Evans et al. 2005), the role of the kidney in ion regulation is less well known, especially at the level of expression and localization of specific ion transport proteins (Marshall and Grosell 2006). Furthermore, the kidney plays an important role in ion regulation of teleosts in both freshwater (FW) and seawater (SW), although renal function may be entirely different in these two environments. FW fish face water loading and ion loss through their permeable body surface, and accordingly, the primary function of the kidney is to excrete excess water and reabsorb filtered solutes. SW fish, by contrast, gain excess ions, lose water by osmosis to their surrounding environment, and consequently ingest SW to prevent dehydration. The primary function of the kidney in

F. Katoh · G. G. Goss (✉)
Department of Biological Sciences, University of Alberta,
Edmonton, Alberta, Canada T6G 2E9
e-mail: greg.goss@ualberta.ca

F. Katoh · R. R. F. Cozzi · W. S. Marshall
Department of Biology, St. Francis Xavier University,
Antigonish, Nova Scotia, Canada

SW is to reabsorb water from the filtrate. The teleost kidney does not exhibit morphological zonation, such as the distinct distribution between cortex and medulla, nor does it have a countercurrent system in the tubular systems (Marshall and Grosell 2006). However, based on both microscopic observation and isolated tubules, the nephron of fishes can be divided into other segments including the glomerulus, proximal tubule, distal tubule (DT), and collecting tubule (CT) (Hickman and Trump 1969).

The $Na^+/K^+/2Cl^-$ cotransporter (NKCC) belongs to the cation Cl^- transporter family and is an integral membrane protein that mediates the electroneutral transport of Na^+, K^+, and Cl^- across epithelial membranes (Haas 1989; Haas and Forbush 2000). Two major isoforms of NKCC have been found in vertebrates, NKCC1 and NKCC2. NKCC1 functions as a secretory isoform that is widely distributed among tissues but basolaterally expressed in all polarized cell types. NKCC2 is thought to function in an absorptive manner and is a kidney-specific isoform that is expressed only on the apical membranes of mammalian kidney cells located in the thick ascending limb of the loop of Henle (TALH; Payne and Forbush 1994; Igarashi et al. 1995; Kaplan et al. 1996; Haas and Forbush 2000).

In fishes, our knowledge of renal NKCC is more limited. Recently, both isoforms, NKCC1 and NKCC2, have been fully or partially cloned in the dogfish (*Squalus acanthias*) rectal gland (NKCC1, U05958, Xu et al. 1994) and kidney (NKCC2, AF521912-AF521917, Gagnon et al. 2002) and in eel (*Anguilla anguilla*; NKCC1, AJ486858; NKCC2, AJ486859; Cutler and Cramb 2002), killifish (*Fundulus heteroclitus*; NKCC1, AY533706; NKCC2, AY533707; Scott et al. 2004), tilapia (*Oreochromis mossambicus*; NKCC1, AY513737, AY513738; NKCC2, AY513739; Hiroi et al. 2005a), Atlantic salmon (*Salmo salar*; NKCC1, AJ417890), and brown trout (*Salmo trutta*; NKCC1, AJ417891; Tipsmark et al. 2002). In addition, NKCC in the kidney of dogfish (Biemesderfer et al. 1996) and sea bass (*Dicentrarchus labrax*; Lorin-Nebel et al. 2006) has been demonstrated by using immunohistochemistry. In gills, the structure responsible for extra renal salt secretion in SW, NKCC distribution has been demonstrated in epithelial mitochondria-rich chloride cells in the mudskipper (*Periophthalmodon schlosseri*; Wilson et al. 2000b), Atlantic salmon (Pelis et al. 2001), Hawaiian goby (*Stenogobius hawaiiensis*; McCormick et al. 2003), tilapia (*O. mossambicus*; Wu et al. 2003), and three different salmonids (*Salvelinus namaycush*, *Salvelinus fontinalis*, and *Salmo salar*; Hiroi and McCormick 2007). NKCC has also been localized in the opercular membrane of killifish (Marshall et al. 2002) and in the yolk-sac membrane of tilapia (Hiroi et al. 2005a, b).

Studies on the nephrons of trout, killifish, and other species have demonstrated distinct functional differences between the tubule segments (Braun and Dantzler 1997) and specific differential localization of transporters (Miyazaki et al. 2002). Nishimura et al. (1983) have shown that, in the distal tubule, chloride efflux (lumen to bath) is significantly higher than chloride influx (bath to lumen), suggesting the net Cl^- reabsorption from the lumen to the bath and with a lumen-positive transepithelial voltage. Thus, the distal tubule of FW fish may act as a reabsorbing segment. The necessity of sodium in addition to chloride to generate the lumen-positive voltage in the distal tubule (Nishimura et al. 1983) suggests the involvement of apical NKCC in Cl^- reabsorption. The differential localization of transporters in teleosts include the cloning and characterization of a kidney-specific chloride channel, OmClC-K, cloned from tilapia (*O. mossambicus*; Miyazaki et al. 2002); OmClC-K mRNA shows elevated transcript levels in FW-adapted tilapia compared with SW-adapted fish, whereas immunohistochemical evidence has revealed OmClC-K located in the basolateral membrane of the distal nephron suggesting that OmClC-K is involved in transepithelial Cl^- reabsorption. In killifish, Cliff and Beyenbach (1992) have reported similarities in the in vitro functional properties of secretory proximal tubules by using isolated SW- and FW-adapted proximal tubules. Their study has shown that SW killifish cannot be distinguished from FW fish on the basis of (1) volume secretion rates, (2) the quantitative composition of secreted fluid with regard to the major osmolytes Na, Cl, Mg, and SO_4, (3) the magnitude and polarity of the transepithelial voltage, (4) the transepithelial permselectivity ratio of Na and Cl, (5) the transepithelial electrochemical potentials of the secreted ions Na, Cl, Mg, and S, and (6) the response of the tubules to the inhibitors ouabain and furosemide (Cliff and Beyenbach 1992). Proximal tubular secretion suggests a functional role for basolateral NKCC.

In this study, we explore mechanisms of teleost salt transport in the gills and kidneys of two different euryhaline fish species by examining the distribution of Na^+/K^+-ATPase and NKCC, two pivotal transport proteins. Our results demonstrate the distinct localization of ion transporters in the osmoregulatory organs (gills and kidneys) between two species and suggest a difference in the ion transport function of fishes with different life histories and strategies.

Materials and methods

Animals

All experiments were conducted under animal care protocols approved by the University of Alberta and St. Francis Xavier University and the Biosciences Animal Policy and

Welfare Committee under the directions provided by the Canadian Council for Animal Care in Canada. All fish were fed daily with commercial fish food, and photoperiod was maintained similar to that of the natural photoperiod in Edmonton, Alberta, Canada or in Antigonish, Nova Scotia, Canada.

Rainbow trout

Adult rainbow trout (*Oncorhynchus mykiss*) of either sex were obtained from Alberta trout growers and held in 450-l indoor tanks with flowing dechlorinated Edmonton tap water (~1.00 mM Na^+, 1.05 mM Ca^{2+}), in the Aquatic Facility of the Department of Biology, University of Alberta, Alberta, Canada. The water temperature was maintained at 11–14°C. Some of the rainbow trout were acclimated gradually (~30%, 50%, 70%, and 90% SW, for 1 week each) to full strength SW (510 mM Na^+, 9.38 mM Ca^{2+}), made using Instant Ocean brand salts (Aquarium Systems, Ohio, USA) in dechlorinated Edmonton tap water, and were maintained for at least 1 week in 190-l circulating indoor holding tanks. We also obtained adult FW rainbow trout of both sexes from Fraser's Mills Fish Hatchery (Antigonish, NS, Canada); these were kept in FW (3.00 mM Na^+, 0.10 mM Ca^{2+}) at the St. Francis Xavier University Animal Care Facility. Some of the rainbow trout were acclimated gradually (~30%, 60%, and 80% SW, for 1 week each) to full strength SW (402 mM Na^+, 8.40 mM Ca^{2+}) and were maintained for 2 weeks in circulating indoor holding tank at 10–12°C.

Killifish

Adult killifish (*Fundulus heteroclitus*) were captured from estuaries near Antigonish, Nova Scotia, Canada, and transported to the Aquatic Facility of the University of Alberta or the Animal Care Facility of St. Francis Xavier University. At the University of Alberta, they were kept in full-strength artificial SW as described above and maintained at least for 1 month in 190-l circulating indoor holding tanks at 15–17°C. Some of the SW killifish were transferred to FW after 1 week of 50% SW pre-adaptation and were then transferred to FW and maintained for at least 2 weeks in a 190-l recirculating FW indoor holding tank. The killifish used for gill tissue sampling at St. Francis Xavier University were second generation from wild-caught parents and were kept in circulating full strength Antigonish SW; some of the fish were then acclimated to FW at least for 2 weeks.

Kidney tissue preparation

Rainbow trout and killifish (*n*=3 each) kept in the Aquatic Facility of the University of Alberta were anesthetized with

MS-222 (1.0 g l^{-1}; Syndel, Canada), and kidneys were immediately dissected. Small pieces (~5 mm slices) of trunk kidney of rainbow trout were removed from the middle and fixed in 4% paraformaldehyde (PFA) in 0.1 M phosphate buffer (PB) for 24 h. The whole trunk kidney of killifish was fixed in 2% PFA-0.2% glutaraldehyde (GA; Electron Microscopy Science, Pa., USA) in 0.1 M PB and in 4% PFA for light microscopy. For transmission electron microscopy (TEM), tissues from both species were fixed in 2% PFA-2% GA, in 0.1 M PB for 24 h, and post-fixed in 1% osmium tetroxide (Electron Microscopy Science) in 0.1 M PB for 1 h. Tissues were also fixed in 2% PFA-0.2% GA in 0.1 M PB for 3 h at 4°C for immunoelectron microscopy.

Gill tissue preparation

Rainbow trout and killifish (*n*=3 each) kept in the Animal Care Facility of St. Francis Xavier University were killed by a sharp blow to the head or by decapitation, respectively. Gill filaments were immediately dissected and fixed in 80% methanol/20% dimethylsulfoxide for 3 h at -20°C for later light-microscopic observations.

Antibodies

The anti-serum (NAK121; Katoh et al. 2000) to Na^+/K^+-ATPase was raised in a rabbit against a synthetic peptide corresponding to a highly conserved region of the Na^+/K^+-ATPase α-subunit of chum salmon (Ura et al. 1996). The monoclonal antibody used to detect the NKCC was concentrate or supernatant of T4 (Lytle et al. 1992) from the Developmental studies Hybridoma Bank, University of Iowa (Iowa city, Iowa, USA). The secondary antibodies used for laser scanning confocal microscopy were either goat anti-mouse IgG or goat anti-rabbit IgG polyclonal conjugated with either Alexa Fluor 488 or Alexa Fluor 594 (Molecular Probes, Ore., USA). Goat anti-mouse IgG and goat anti-rabbit IgG conjugated with 10-nm or 5-nm gold particles and the silver enhancing kit were obtained from British Bio Cell International (UK).

Kidney: light microscopy, immunocytochemistry, and quantitative analysis

Kidney tissues from both species were dehydrated in ethanol and embedded in Paraplast (Thermo Electron, Mass., USA). Serial sections cut at a thickness of 4 μm were divided into two groups and mounted on polylysine-coated slides (Sigma) for immunocytochemistry. The deparaffined sections were incubated sequentially with (1) 2% normal goat serum (NGS) for 30 min, (2) anti-Na^+/K^+-ATPase serum diluted at 1:4,000 or anti-NKCC (T4, concentrate) diluted at 1:6,000 in T-PBS (2% NGS, 0.1%

bovine serum albumin [BSA], 0.01% NaN$_3$, 0.02% keyhole limpet hemocyanin in 0.01 M PBS), (3) goat anti-rabbit 5-nm gold (to Na$^+$/K$^+$-ATPase) or goat anti-mouse 5-nm gold (to NKCC) diluted 1:50 with PBS containing 1% BSA for 30 min at room temperature. The gold particles occurring at the location of each antibody were emphasized with the silver-enhancing kit after incubation for 15 min at 20°C. In addition, serial sections were stained with periodic acid/Schiff (PAS), and nuclei were counterstained with hematoxylin to examine the general morphology of trunk kidney. The sections were dehydrated in series of ethanol and xylene, mounted with Permount (Fisher Scientific, Canada), and observed under a light microscope (Leica DMRXA, Germany/Nikon Microphot FXA, Japan).

For quantitative analysis of renal tubules of both species, the number of all tubules appearing in the image frames (~0.27 mm^2) was counted in at least four images per animal ($n=3$), and the appearance of each segment (%) was calculated for fish in FW and SW. Significant differences in the appearance of each segment were analyzed by using the χ^2 test.

Kidney: TEM

After dehydration in ethanol, the kidneys of both species were transferred to propylene oxide and embedded in Spurr's resin (Polysciences, Pa., USA). Ultrathin sections were cut with a diamond knife, mounted on grids, stained with uranyl acetate and lead citrate, and observed with a transmission electron microscope (Philips model 201, Philips, Netherlands).

Kidney: immuno-TEM

Kidneys of both species fixed for immuno-TEM were dehydrated up to 100% ethanol and embedded in LR white resin (London Resin, UK). Ultrathin 80-nm sections (gold sections) were cut with a diamond knife, mounted on grids, and incubated sequentially with (1) filtered T-PBS for 10 min at room temperature, (2) primary antibody, viz., NAK121 at 1:100 or T4 concentrate at 1:100 in T-PBS overnight at 4°C, and (3) secondary antibody, viz., goat anti-rabbit 10-nm gold (to NAK121) or goat anti-mouse 10-nm gold (to T4) in PBS for 2 h at room temperature. They were then counterstained with uranyl acetate and lead citrate and observed with a transmission electron microscope (Philips model 201, Philips).

Gill immunocytochemistry and confocal laser scanning microscopy

Fixed gill tissues from both species were dehydrated in ethanol and embedded in Paraplast. Serial sections cut at a thickness of 4 μm were mounted on polylysine-coated slides for immunocytochemistry. The deparaffined sections were incubated sequentially in (1) 2% NGS for 30 min at room temperature, (2) anti-Na$^+$/K$^+$-ATPase serum diluted at 1: 1000 and anti-NKCC (T4 supernatant) diluted at 1:100 in blocking buffer (2% NGS, 0.1% BSA, 0.01% NaN$_3$ in 0.01 M PBS) overnight at 4°C, and (3) goat-anti rabbit Alexa Fluor 594 and goat-anti mouse Alexa Fluor 488 diluted at 1:500 with T-PBS for 4 h at room temperature. After three final rinses, the sections were mounted in mounting medium (Geltol, Immunon Thermo Shandon, Pa., USA). Slides were viewed by using a laser scanning confocal microscope (Olympus, model FV300, ON, Canada).

Results

Light-microscopic observations of kidney tubules in killifish and rainbow trout

In both killifish and rainbow trout kidney, the nephron could be clearly classified into differentiated segments by using standard morphological characteristics. These included the renal corpuscle, the first (PI) and second (PII) segments of the proximal tubules, and the DT and CT (see Figs. 1, 2, 3). In killifish, PI could be clearly identified as PAS-positive tubules, whereas PII tubules were PAS-negative and displayed apically oriented nuclei (Fig. 1e) by light microscopy. The PAS staining method was used to label the proximal tubules as this segment has a brush border coated with a glycocalyx. Rainbow trout PI segment was also identified by the well-developed PAS-positive microvilli in the lumen. The PI segment in both killifish and rainbow trout showed vesicle-like structures in the apical region (arrows in Fig. 1e,f) corresponding to the lysosomes and pinocytotic vesicles observed under TEM (see next section). DT in killifish could be identified as PAS-positive, but the nuclei in this segment did not appear to be regularly oriented in the apical region of the cell (Fig. 1g). On the other hand, in rainbow trout, the DT was classified by its PAS-negative lumen and generally smaller diameter than the proximal segments (Fig. 1h). The CT in both species was recognizable by the basally oriented nuclei and the thin muscle layer around the tubules (Fig. 1g,h). Based on the number of distinct tubule sections per image analyzed, we determined that the nephron of killifish was composed of long proximal tubules (94% of total length for SW renal tubule; 87% for FW renal tubule; Table 1) with a short DT (5% for SW; 6% for FW; Table 1). In contrast, the rainbow trout kidney in both FW and SW possessed relatively short proximal tubules (29% for SW; 31% for FW; Table 1) and longer DT (63% for SW; 64% for FW; Table 1). Killifish

Fig. 1 Periodic acid/Schiff-stained light micrographs of seawater (SW)-acclimated killifish (**a**, **c**, **e**, **g**) and freshwater (FW)-acclimated rainbow trout (**b**, **d**, **f**, **h**) trunk kidneys (*G* glomeruli, *PI* first segment of proximal tubules, *PII* second segment of proximal tubules, *DT* distal tubules, *CT* collecting tubules). Non-labeled tubules are the second segment of proximal tubules in **a**, **b**. *Arrows* in **e**, **f** indicate pinocytotic vesicles and lysosomes in the sub-apical region of the cells in PI. *Bars* 100 μm (**a**, **b**), 50 μm (**c-h**)
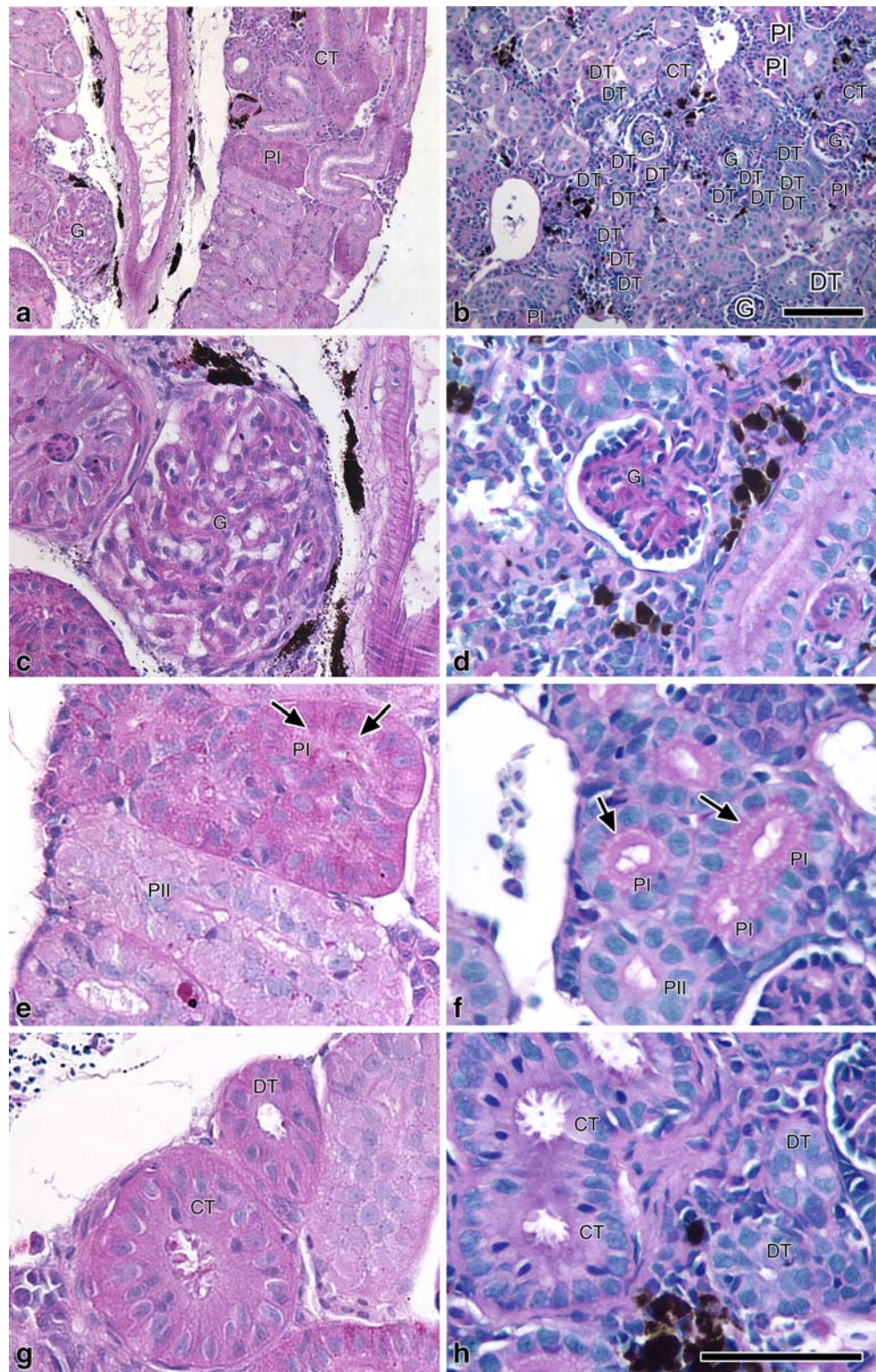
glomeruli were large and found less frequently than in rainbow trout in the sections examined (Fig. 1a-d, Table 1). In both species, no significant differences were observed in the appearance of the segments between SW- and FW-adapted animals.

Electron-microscopic observations of kidney tubules in killifish and rainbow trout

Examination by electron microscopy revealed that all epithelial cells in every segment of the renal tubule had a

rich population of mitochondria and a distinct basolateral tubular system as common fine structures. However, the three identified segments of the tubules (PI, PII, and DT) were characterized by distinct ultrastructural differences in each species. Cells in the PI segment in killifish (Fig. 2a-c) had apical microvilli that extended far into the tubular lumen. Specifically, these cells had distinct sub-apical vesicles, epinuclear pinocytotic vesicles, and lysosomes in the sub-apical region of the cells (Fig. 2, arrowheads, stars, ly). The basolateral membrane was clearly visible in the PI segment (Fig. 2c). Cells in the PII segment (Fig. 2d-f) in killifish did not possess pinocytotic vesicles nor did they have electron-dense sub-apical vesicles, as was typical of the PI segment (Fig. 2a,b). The DT segment could be distinguished from the PI and PII segments as they possessed a much more developed basolateral membrane and more elongate mitochondria (Fig. 2g-i). The basolateral membrane lay in close apposition with these mitochondria and extended throughout the cellular cytoplasm. This was in contrast to the PI and PII segments where the basolateral membrane did not extend throughout the cell, and the mitochondria were shorter.

In trout, similar distinctions between the segments were observed, as found in the killifish above. The PI segment contained numerous sub-apical vesicles and pinocytotic vesicles, and the basolateral membrane, although appearing more convoluted than in killifish, did not extend into the apical region of the cell (Fig. 3a-c). In the PII segment, no pinocytotic vesicles or sub-apical vesicles were seen, similar to the killifish PII (Fig. 3d-f). The DT in trout also possessed very long mitochondria in close apposition to the extensive network of basolateral membrane (Fig. 3g,h,j). The junctions between the mitochondria-rich cells in the renal tubules were tight in both SW and FW animals of both species.

For the two species, we also examined the kidney ultrastructure in both SW- and FW-adapted individuals and found no remarkable differences in its fine structure. Of note, in many of the samples, the primary cilia with their classic 9+2 structure were apparent in the the tubular lumen of the PI, PII, and DT segments (Fig. 3i).

Tissue distribution of Na^+/K^+-ATPase and NKCC

No differences were found in the NKCC immunolocalization patterns of kidneys between SW- and FW-acclimated fish in either species. The T4 antibody has been shown to be specifically immunoreactive to NKCC from many vertebrates including teleost fishes (Lytle et al. 1995; Wilson et al. 2000b; Pelis et al. 2001; Marshall et al. 2002; McCormick et al. 2003; Wu et al. 2003; Hiroi et al. 2005a, b). Although the unreliability of T4 should be noted in its application in some tissues (Zhang et al. 2007), the

Fig. 2 Transmission electron micrographs of the first segment of the proximal tubule (**a-c**), the second segment of the proximal tubule (**d-f**), and the distal tubule (**g-i**) of SW-acclimated killifish; the apical region (**b**, **e**, **h**) and cytoplasmic area (**c**, **f**, **i**) of cells in the each segment are shown at higher magnification (*t* tubular lumen, *m* mitochondria, *v* microvilli, *n* nuclei, *b* basolateral membrane, *ly* lysosomes, *stars* pinocytotic vesicles, *arrowheads* sub-apical vesicles). *Bars*, 5 μm (**a**, **d**, **g**); 1 μm (**b**, **c**, **e**, **f**, **h**, **i**)

immunospecificity of the T4 antibody for ion-transporting cells in fish has been well confirmed. In both killifish (Fig. 4a,b) and rainbow trout trunk kidneys (Fig. 4c,d), the tissue distribution of Na^+/K^+-ATPase and NKCC was examined with immunocytochemistry by using anti-Na^+/K^+-ATPase and anti-NKCC antibodies, respectively (see the adjacent serial sections in Fig. 4a–d for a close comparison). Na^+/K^+-ATPase immunoreactivity was detected in the basolateral membrane of every tubule in the trunk kidneys in both killifish (Fig. 4a) and rainbow trout (Fig. 4c). However, the intensity and pattern of staining in each of the segments served as a specific marker for each segment. The staining in PI was much less intense than that in the PII segment. Furthermore, the staining in both these segments of the kidney appeared to be in lower regions of the basolateral membrane (cytoplasm). However, the staining in the DT was more intense than that in PI, and in contrast to that seen in PI and PII, the staining pattern appeared throughout the cell. Staining for NKCC (Fig. 4b,d) revealed the greatest difference between the two species. In the killifish kidney, NKCC immunoreactivity was detected in the basolateral membrane of the PII segment and in the apical region of the DT and CT (Fig. 4b). On the other hand, NKCC staining in trout was found apically located in the DT and CT and was absent in the PII segment (Fig. 4d).

TEM immuno-gold labeling in kidneys

Using TEM immuno-gold labeling, we revealed a distinct difference in the distribution of NKCC in kidneys between killifish and rainbow trout. In killifish trunk kidney, Na^+/K^+-ATPase immuno-gold labeling confirmed the basolateral membrane localization of this protein in these cells (Fig. 5a). We found that NKCC was preferentially localized on the basolateral membrane in the PII segment (Fig. 5b). However, we also detected a small amount of signal on the apical surface (Fig. 5c). The NKCC signal in killifish DT was strong in the apical membrane (Fig. 5d) of the cells but was scarcely detectable in the basolateral membrane (Fig. 5e). In rainbow trout trunk kidney, Na^+/K^+-ATPase was used to identifiy positively a region as basolateral (Fig. 6a) with abundant Na^+/K^+-ATPase reactivity. NKCC immunoreactivity in trout was detected only in the apical membrane of the DT (Fig. 6b), and not in the basolateral
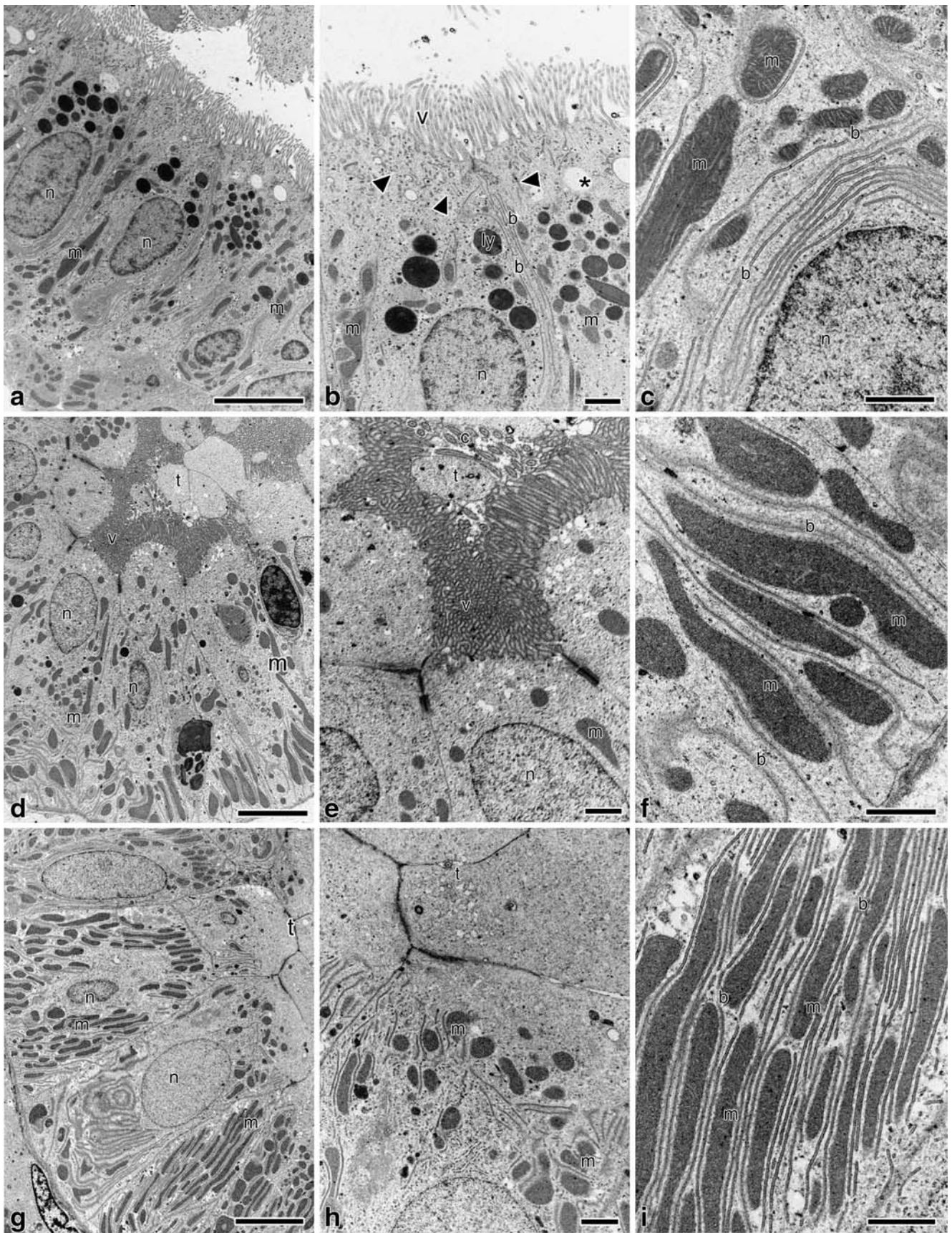
membrane of the same segment (Fig. 6c) or in other segments (data not shown).

Immunocytochemistry in gill filaments

In contrast to the immunolocalizations of NKCC transporter in killifish and rainbow trout kidneys, we found striking differences in the distribution of NKCC between FW- and SW-acclimated fish in gill filaments whose architecture is presented in Fig. 7h. In FW killifish, NKCC was localized in the apical area of Na$^+$/K$^+$-ATPase-positive mitochondria-rich cells (Fig. 7a-c). In SW killifish, NKCC was instead colocalized with Na$^+$/K$^+$-ATPase in the basolateral membrane of the mitochondria-rich cells (Fig. 7d-g). Because the mitochondria-rich cells possessed an intricate tubular system formed by extensive invaginations of the basolateral membrane (Evans et al. 2005), immunostaining of basolateral membranes appeared all across the cell body. In FW rainbow trout gill filaments, most of the population of Na$^+$/K$^+$-ATPase-positive mitochondria-rich cells was located in filaments (Fig. 8a). We found that mitochondria-rich cells in rainbow trout gill had three different populations: (1) Na$^+$/K$^+$-ATPase-positive, (2) NKCC-positive, and (3) both Na$^+$/K$^+$-ATPase- and NKCC-positive cells. Interestingly, the cells of population (3) were found mostly in the lamellae of FW rainbow trout gills (Fig. 8b-d), whereas SW-acclimated rainbow trout gills had the most immuno-positive cells located in the gill filament (Fig. 8e-h). The trailing edge of the filament, the focus of most studies of mitochondria-rich cells, possessed Na$^+$/K$^+$-ATPase-positive but NKCC-negative mitochondria-rich cells. However, in the region between and at the root of the gill lamellae, we found mitochondria-rich cells with positive staining for both Na$^+$/K$^+$-ATPase and NKCC. We only observed a few mitochondria-rich cells with single Na$^+$/K$^+$-ATPase-positive labeling in the lamellae (Fig. 8g).

Discussion

The kidneys, gills, and intestines are the main osmoregulatory organs in teleosts (Evans 1979). Whereas the morphology and physiology of branchial mitochondria-rich chloride cells have been well studied, renal ion transport mechanisms are less well understood (Evans et al. 2005; Marshall and Grosell 2006). Primarily, this has been attributed to the relative complexity of the kidney and difficulties in examining this tissue. We have examined, in detail at the light-microscopic and electron-microscopic levels, the morphology and localization of salt (Na$^+$ and Cl$^-$) transporters (Na$^+$/K$^+$-ATPase and NKCC) in the kidney and gills in the two species. This study is the first to report the differential localization of NKCC protein in the renal

Fig. 3 Transmission electron micrographs of the first segment of the proximal tubule (**a-c**), the second segment of the proximal tubule (**d-f**), and the distal tubule (**g-j**) of FW-acclimated rainbow trout; the apical region (**b, e, h**) and cytoplasmic area (**c, f, j**) of cells in the each segment are shown at higher magnification (*t* tubular lumen, *m* mitochondria, *v* microvilli, *n* nuclei, *b* basolateral membrane, *ly* lysosomes, *stars* pinocytotic vesicles, *arrowheads* sub-apical vesicles). Primary cilia (**i**) from a different section of rainbow trout distal tubule lumen show the clear 9+2 structure. *Bars* 5 μm (**a, d, g**), 1 μm (**b, c, e, f, h, j**), 0.5 μm (**i**)

tubules, with an examination of gill function, of two euryhaline species having different preferences with respect to environmental osmolality. The results indicate that killifish and rainbow trout have evolved remarkably different strategies regarding kidney and gill functions to survive in SW and FW. This study also clearly outlines morphological characteristics that can be used to differentiate these renal segments in each of these species.

Kidney morphology

In fish, the kidney consists of two primary compartments, the head kidney and the trunk kidney (Hickman and Trump 1969). Embryologically, the head kidney and trunk kidney are derived from the pronephros and mesonephros, respectively (Romer and Parsons 1977). The head kidney is the anterior portion of the kidney and probably has no renal function (Braun and Dantzler 1997) as it consists primarily of lymphoid tissue, whereas the trunk kidney is composed of many nephrons and interstitial lymphoid tissue (Hickman and Trump 1969). Our observations have specifically dealt with the morphology and function of the trunk kidney. With regard to basic structure and morphology, fish kidneys are distinctly different from mammalian kidneys in that they do not display zonation, and the nephrons of teleosts are devoid of the loop of Henle (Hendricks 1983; Yokote et al. 1995; Braun and Dantzler 1997). In the present study, light microscopy has demonstrated distinct features of each tubule type in killifish and rainbow trout trunk kidneys, whereas TEM has revealed the ultrastructure of each segment of the nephron. In both of the species examined, viz., rainbow trout and killifish, each segment of the renal tubule exhibits similar structural features. Primary cilia that occur in the PI, PII, and DT in both species are generally found in fish renal tubules (Yokote et al. 1995) and have been reported as mechano- and chemo-sensors in vertebrate cells (Praetorius and Spring 2005). The morphology of rainbow trout kidney is consistent with previously published findings (Katoh et al. 2006). The mitochondria-rich nature of the cells in all the renal tubules and the extensive microvilli and lysosomes in the PI segment seem to be well-conserved ultrastructures from fishes to mammalian kidneys (Hickman and Trump 1969; Mandal and Wenzl 1979). Edwards and Schnitter
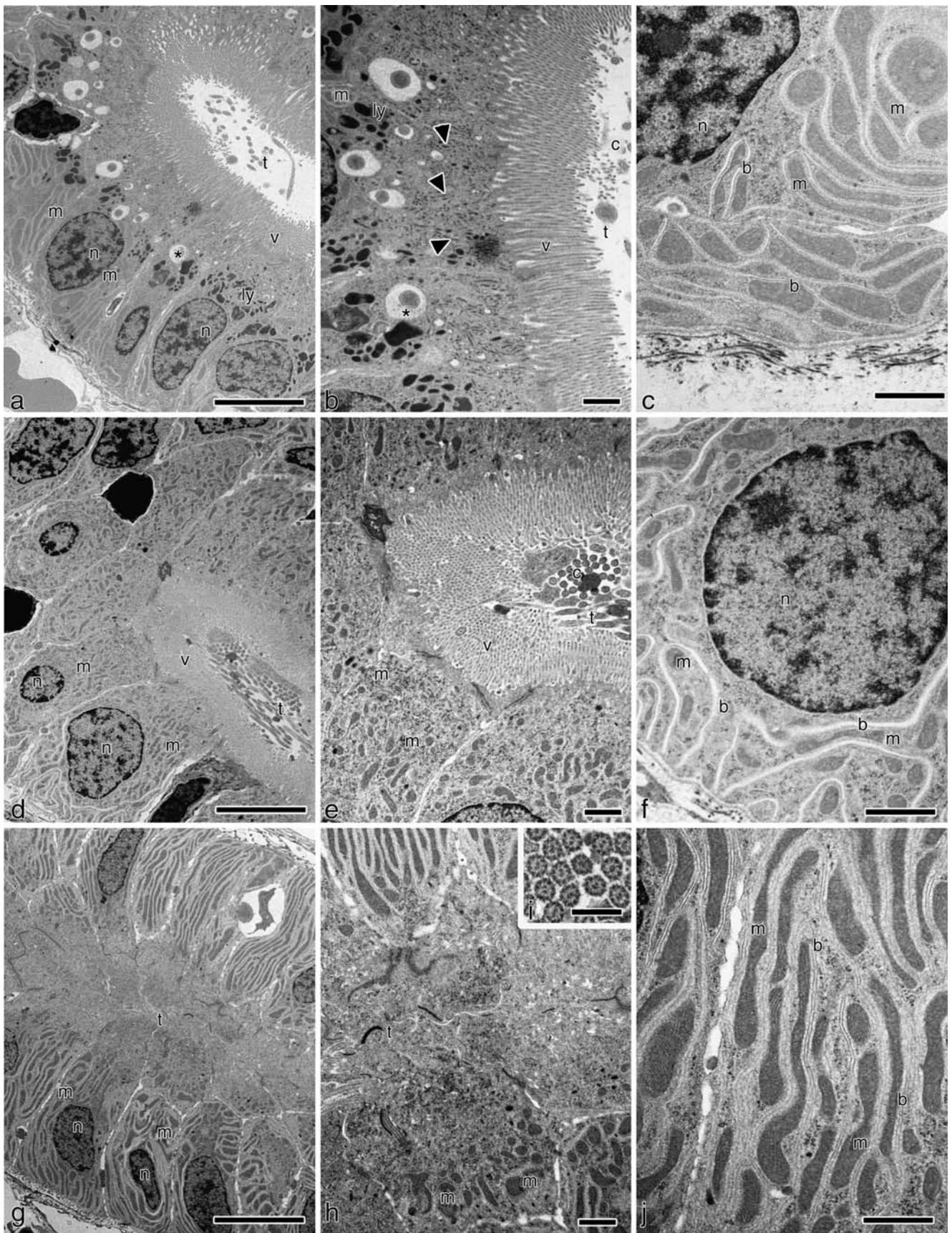
Table 1 Relative length (%) of each segment of a renal tubule (*PI* first segment of proximal tubule, *PII* second segment of proximal tubule, *CT* collecting tubule, *DT* distal tubule, *SW* seawater, *FW* freshwater)

	PI	PII	DT	CT	Glomerulus
Killifish					
SW	43	51	5	4	2
FW	33	54	6	5	3
Rainbow trout					
SW	15	13	63	8	5
FW	16	15	64	4	4

(1933) have previously reported that killifish have a relatively large and well-vascularized glomerulus and suggest that the proximal convoluted tubule constitutes about nine-tenths of the length of the renal tubule. The finding that killifish proximal tubule comprises ~90% of total nephron length has been confirmed by Cliff and Beyenbach (1988) in their physiological study by using isolated renal tubules of FW-adapted killifish. Our observation of light-microscopic preparations (summarized in Fig. 9) in this study are consistent with these previous reports; the killifish kidney sections show the same tendency exhibiting a much greater proportion of their total tubule length as the proximal segment (PI and PII).

Consequently, we have seldom found sections of the DT (Table 1) in our light-microscopic preparations.

In the present study, no morphological differences in kidneys between FW- and SW-adapted animals are apparent for the variables tested in either of species (Table 1). However, our results in this study differ from those of other species such as the European eel (Olivereau and Olivereau 1977) and American eel (Graffin 1937). The kidney of the European eel (*Anguilla anguilla*) shows a significant reduction in the height and nuclear size of the tubular epithelial cells during the first two days after transfer from FW to SW (Olivereau and Olivereau 1977). Following the transfer to SW, a rapid increase over 2 days followed by a decrease over 5 days also occurs in cell height and nuclear size (Olivereau and Olivereau 1977). Additionally, seasonal histological alteration has been reported in the American eel, *Anguilla rostrata*, caught in either salt or brackish water. Granular cells can be found in the proximal convoluted segment in kidney in winter *A. rostrata*, but not in summer animals (Grafflin 1937).

Ion transporter distribution in renal tubules

Interestingly, in both killifish and rainbow trout, adaptation to either FW or SW do not induce any apparent immuno-histochemical alterations in the kidney at either the light- or

Fig. 4 Light-microscopic images of Na$^+$/K$^+$-ATPase immunocytochemistry (**a**, **c**) and Na$^+$/ K$^+$/2Cl$^-$ cotransporter (NKCC) immunocytochemistry (**b**, **d**) in SW-acclimated killifish (**a**, **b**) and FW-acclimated rainbow trout (**c**, **d**). Note the differential staining of the various segments (*PI* first segment of proximal tubules, *PII* second segment of proximal tubules, *DT* distal tubules, *CT* collecting tubules). Detailed localization is presented in immuno-transmission electron micrographs in Figs. 5, 6. *Bar* 100 μm
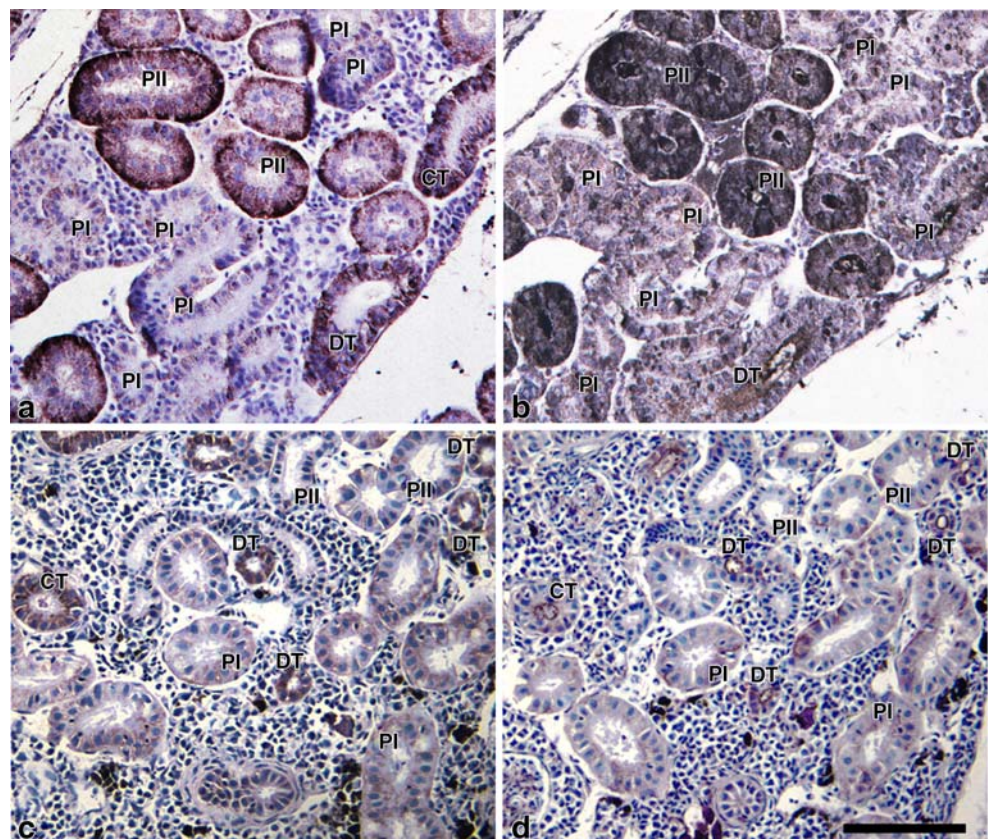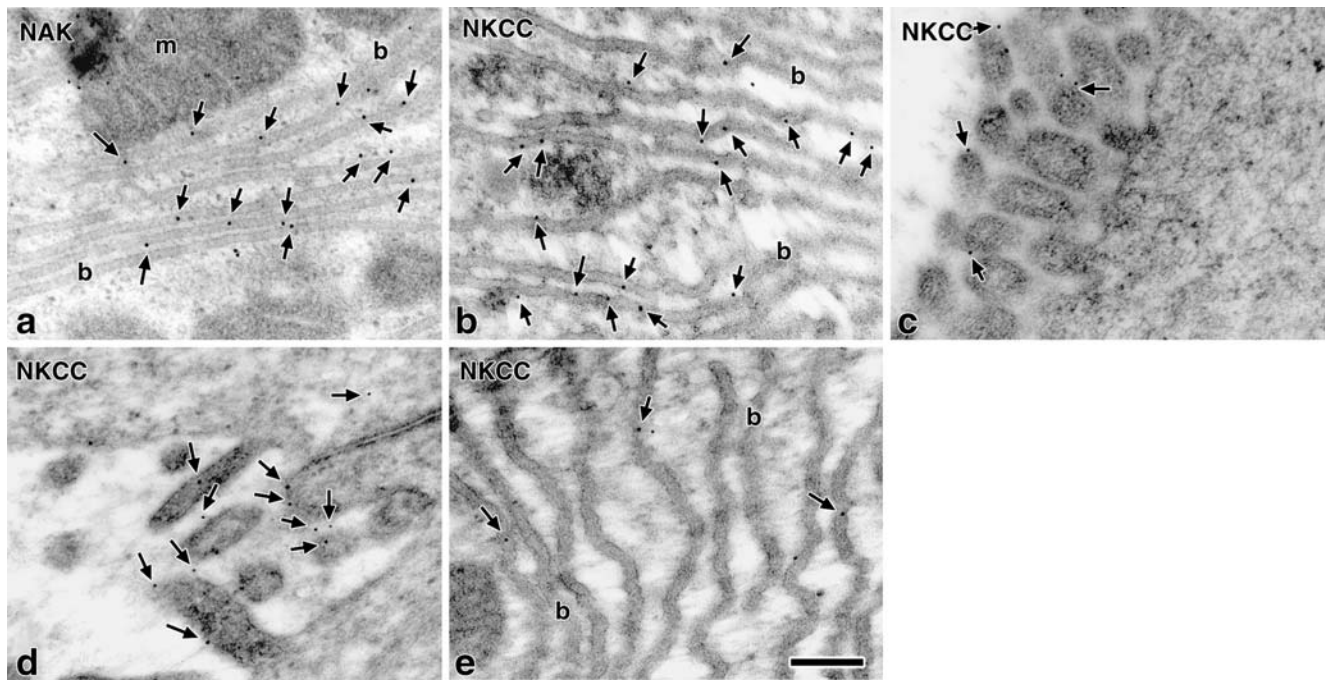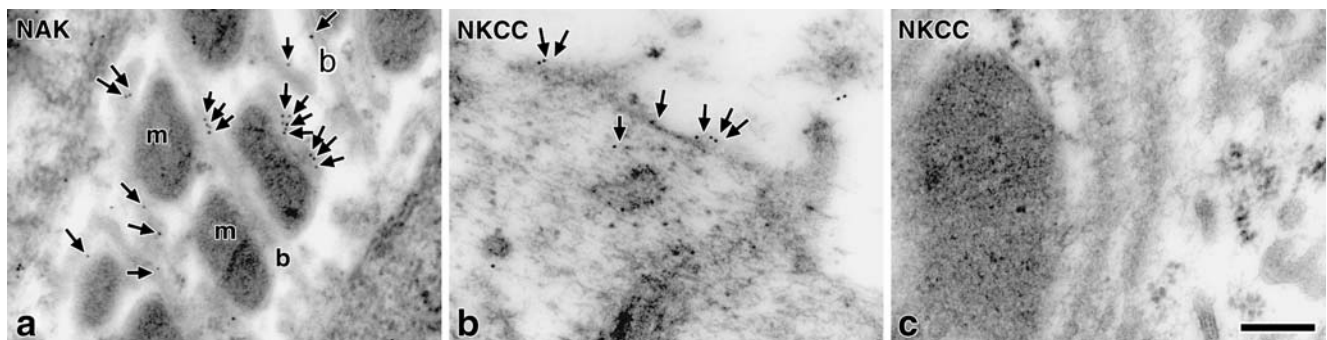
Fig. 5 Immuno-transmission electron micrographs of SW-acclimated killifish kidney tubules (*arrows* localization of secondary antibodies conjugated with immuno-gold particles, *m* mitochondria, *b* basolateral membrane). Na$^+$/K$^+$-ATPase (*NAK*) was distributed in the basolateral membrane of the second segment of the proximal tubules (**a**). Na$^+$/K$^+$/ 2Cl$^-$ cotransporter (*NKCC*) was localized in the basolateral membrane of the second segment of proximal tubules (**b**) and distal tubules (**e**). Apical localization of NKCC was detected strongly in distal tubules (**d**) and weakly in the second segment of proximal tubules (**c**). *Bar* 200 nm

electron-microscopic level. Two major isoforms of the NKCC, the secretory form NKCC1 and the absorptive form NKCC2, are found in vertebrates. Generally speaking, in mammals, NKCC2 is reported as a kidney-specific isoform and is apically located only in the TALH (Payne and Forbush 1994; Igarashi et al. 1995; Kaplan et al. 1996; Haas and Forbush 2000). In dogfish kidney, however, the basolateral isoform (NKCC1) has been observed to be distributed in the proximal tubules and the apically located isoform (NKCC2) is present from the proximal tubule to the CT (Biemesderfer et al. 1996). The secreting isoform (NKCC1) has also been found basolaterally in the dogfish rectal grand (Lytle et al. 1992). The anti-NKCC antibody (T4) used in the present study has been shown to recognize both secretory and absorptive isoforms in a diverse variety of animal tissues (Lytle et al. 1995). Thus, it is not possible to make a firm description of which isoform is present. However, in keeping with current findings in mammalian systems, we suggest that the killifish kidney has both an apically located NKCC2 and a basolaterally located NKCC1, whereas rainbow trout kidney expresses only apically located NKCC2 (Fig. 9).

Fig. 6 Immuno-transmission electron micrographs of FW-acclimated rainbow trout distal tubule. Immunolocalization of Na$^+$/K$^+$-ATPase (*NAK*; **a**, *arrows*) in the basolateral membrane and Na$^+$/K$^+$/2Cl$^-$ cotransporter (*NKCC*; **b**, *arrows*) in the apical membrane of cells in the distal tubules (*m* mitochondria, *b* basolateral membrane). NKCC was negative in the basolateral membrane of the distal tubules (**c**). *Bar* 200 nm

Fig. 7 Na$^+$/K$^+$-ATPase (*red*) and NKCC (*green*) immunohistochemistry in gills of FW-acclimated killifish (**a-c**) and SW-acclimated killifish (**d-g**). Whole-mount images (**a, b**) show the apical localization of NKCC in Na$^+$/K$^+$-ATPase-positive mitochondria-rich cells. In a paraffin section (**c**), the NKCC is clearly localized in apical crypts (*arrows*). In SW-acclimated fish, NKCC (**d**, *green*) colocalizes with Na$^+$/K$^+$-ATPase (**e**, *red*) in the basolateral membrane of mitochondria-rich cells. The merged view (**f**) shows the clear colocalization (*yellow*). **g** Higher magnification view of the *boxed area* in **f**. **h** Representation of the gill filament architecture (*red arrows* direction of water flow, *TL* trailing edge of gill filament, *LD* leading edge of gill filament, *F* filaments, *L* lamellae, *MRC* mitochondria-rich cells, *A* afferent filament artery, *E* efferent filament artery). *Bars* 100 μm (**a, b, d, e, f**), 10 μm (**c, g**)
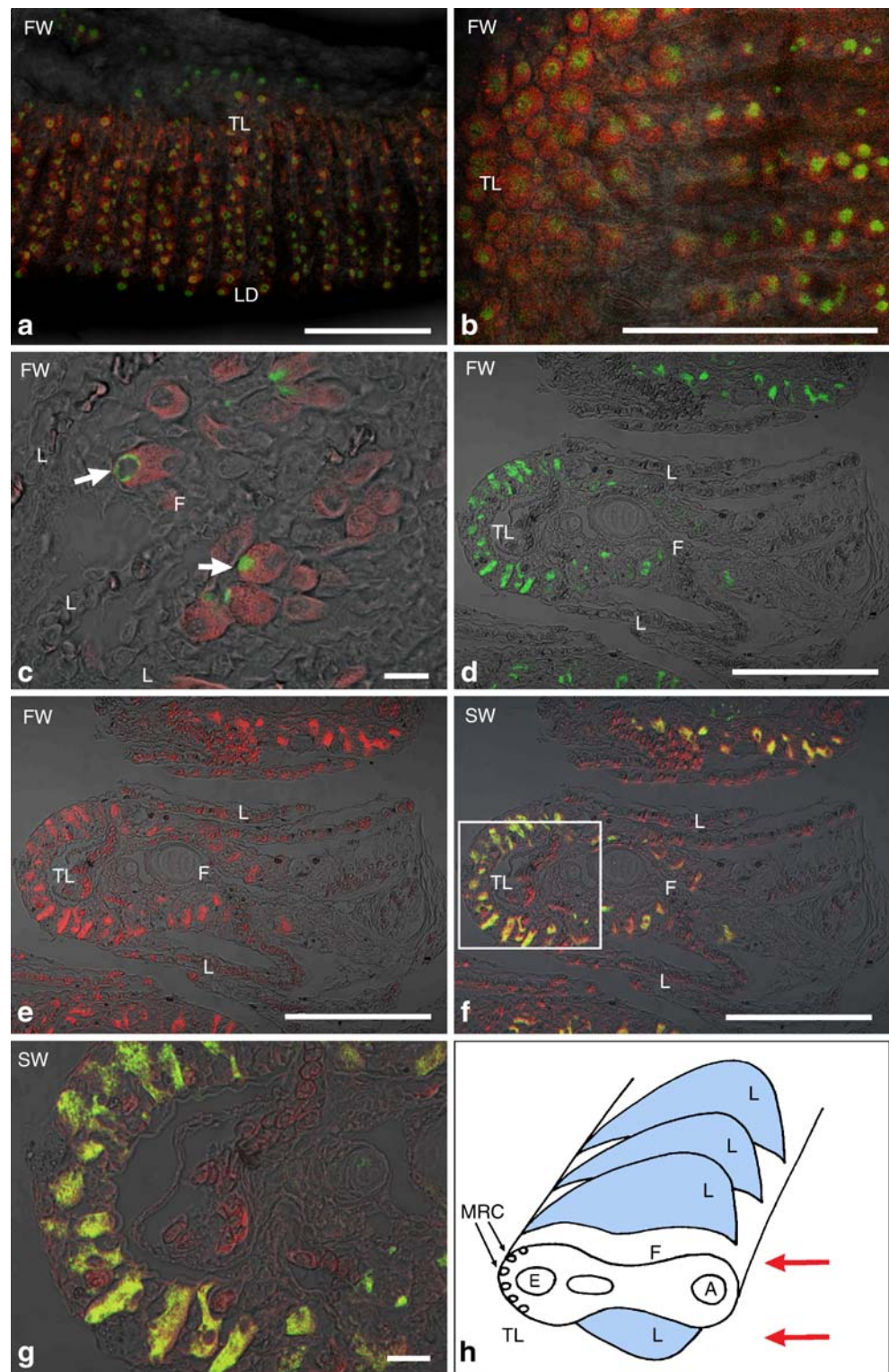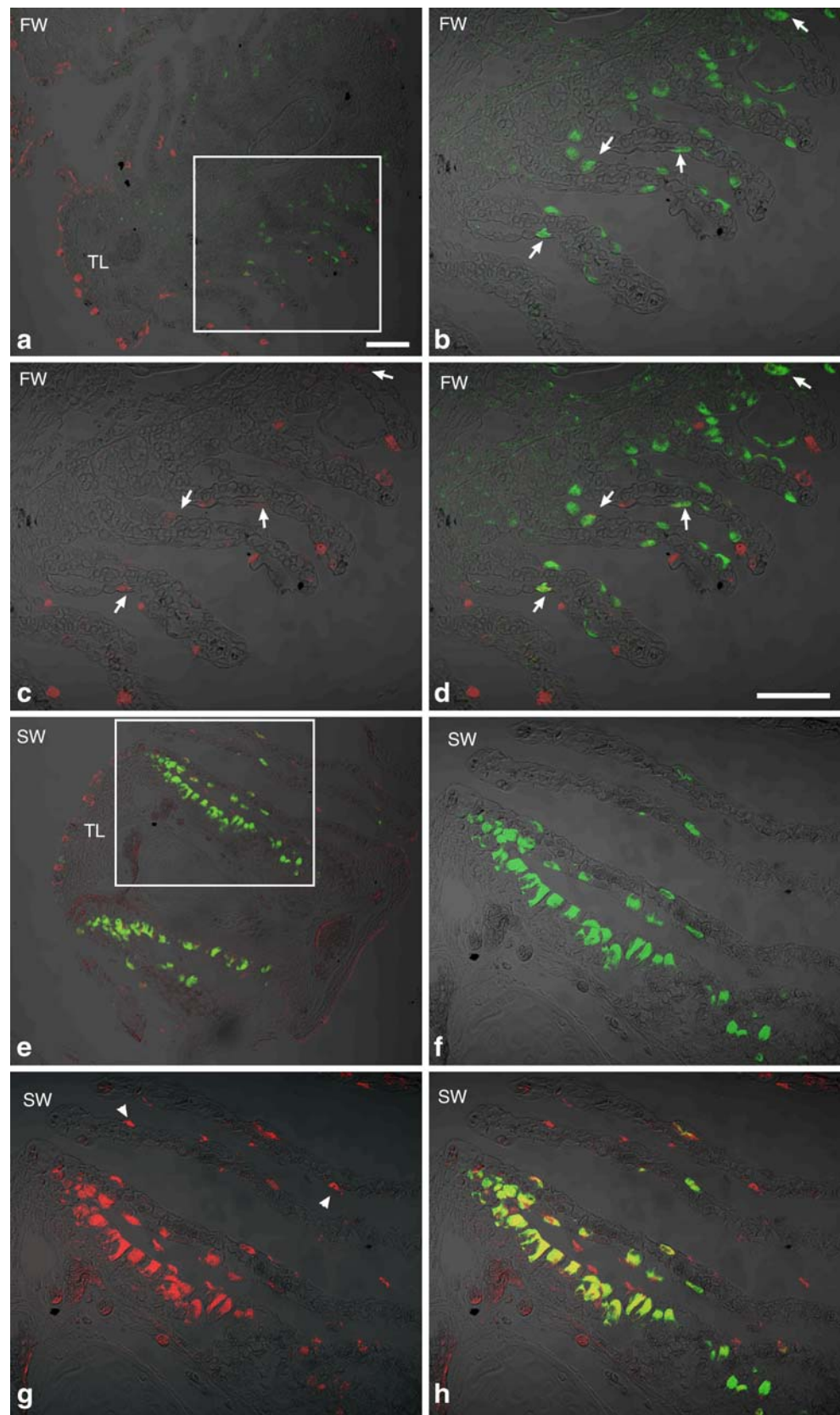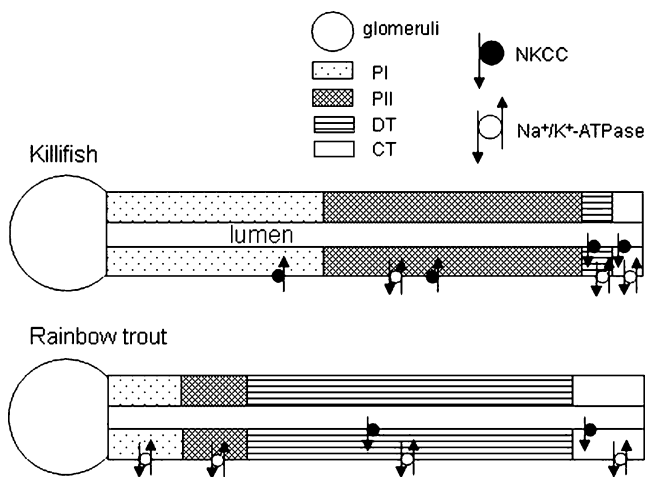

Proximal tubule

Cliff and Beyenbach (1992) have reported similar functional properties of secretory proximal tubules isolated from both SW- and FW-adapted killifish; these are consistent with our findings. In their study, although the fluid

secretion rate is higher in SW than in FW fish, no significant difference has been seen in the concentrations of ions in the exudates. Our present findings agree with their physiological analysis, i.e., that, in killifish, the PII possesses both Na$^+$/K$^+$-ATPase and the secretory isoform of NKCC in the basolateral membrane of renal mitochondria-

Fig. 8 Immunohistochemistry of Na$^+$/K$^+$-ATPase (*red*) and NKCC (*green*) in gills of FW-acclimated (**a-d**) and SW-acclimated (**e-h**) rainbow trout. **b–d** Higher magnification views of *boxed area* in **a**. In FW fish, Na$^+$/K$^+$-ATPase-positive cells are mainly localized in trailing edge (**a**, *TL*) of the filament, and NKCC is localized in the cells distributed in the lamellae (**a, b**; *arrows* in **b**). Fewer cells are Na$^+$/K$^+$-ATPase-positive in the lamellae (**c, d**) in FW (*arrows* cells possessing both Na$^+$/K$^+$-ATPase and NKCC in lamellae). **f–h** Higher magnification views of *boxed area* in **e**. SW-acclimated rainbow trout have Na$^+$/K$^+$-ATPase-positive cells (*red*) in the trailing edge (*TL*) of the gill filament and mostly in the area between and roots of lamellae (**g**, *red*). The Na$^+$/K$^+$-ATPase-positive cells distributed between the roots of lamellae are also NKCC-positive cells (**f**), and the two transporters are colocalized (*yellow* in merged image in **h**). Note the Na$^+$/K$^+$-ATPase-positive but NKCC-negative cells in lamellae (*arrowheads*). *Bars* 50 μm

Fig. 9 Summary of histological features and localization of Na$^+$/K$^+$-ATPase and Na$^+$/K$^+$/2Cl$^-$ cotransporter (*NKCC*) in the kidney of killifish and rainbow trout (*closed circles* NKCC, *open circles* Na$^+$/K$^+$-ATPase, *PI* first segment of proximal tubule, *PII* second segment of proximal tubule, *DT* distal tubule, *CT* collecting tubule). Relative proportions represent the relative length of each segment as shown in Table 1

rich cells. The basolaterally located NKCC in the killifish PII may function as part of a fluid secretory pathway via a standard model whereby the transport of Na$^+$/K$^+$ and Cl$^-$ from the extracellular fluid into the cell results in apical Cl$^-$ secretion via apically oriented Cl$^-$ channels, and Na$^+$ is exported because of the colocalized basolateral Na$^+$/K$^+$-ATPase and transverses passively into the lumen via a paracellular pathway (Hickman and Trump 1969; Beyenbach 1995). In isolated renal proximal tubules from other marine species, such as elasmobranch and winter flounder, net Na$^+$ and Cl$^-$ secretion has also been observed (Beyenbach and Frömter 1985; Beyenbach et al. 1986); the secretion is stimulated by cAMP and inhibited by ouabain and furosemide. The net secretion of NaCl in the proximal tubule in both SW and FW environments is probably a conserved function within marine euryhaline teleost species (Braun and Dantzler 1997). Beyenbach and Liu (1996) have suggested that active transepithelial secretion of Mg^{2+} is an important driving force for Na$^+$, Cl$^-$, and water secretion, and that Na$^+$ and Cl$^-$ move across the epithelium by paracellular pathways. Dantzler (2003) has reviewed salt transport in the proximal tubule of a variety of animals and suggested that NKCC is involved in the transcellular Cl$^-$ secretion with entry of Cl$^-$ at the basolateral membrane of proximal tubules (Dantzler 2003). The PI has been suggested to be a salt-reabsorbing segment in both FW species (Nishimura and Imai 1982; Marshall and Grosell 2006) and marine teleosts (Nishimura and Imai 1982). In this study, the basolateral NKCC has been shown to be immunohistochemically present in killifish PII but absent from cells in the PI segment of both killifish and rainbow

trout. Thus, if salt uptake occurs in the PI, it does not involve apical NKCC. In their review, Braun and Dantzler (1997) report that the Cl$^-$/HCO$_3$ exchanger, Na$^+$/H$^+$ exchanger, and Na$^+$/glucose cotransporter could participate in this salt-reabsorbing process, but further analysis is needed to confirm whether these transporters exist in the proximal tubules of killifish and rainbow trout.

Using immuno-TEM, we have demonstrated that killifish PII exhibits apical NKCC staining, although it is much weaker than that in the basolateral membrane of the same cells. This segment may therefore act as either an absorbing (using the apical NKCC) or secreting (using basolateral NKCC) segment as a mechanism to deal with the rapid environmental salinity changes that killifish commonly experience in their natural habitat, assuming the apical and basolateral transporters are regulated differently. The length of the proximal tubules of the trunk kidney in rainbow trout is about 30% of the total renal tubule (measured as sections counted), and immunoreactivity for NKCC is not detectable in the proximal segments. These observations indicate that the long PII of killifish with its basolateral NKCC (>50% of whole length of renal tubules) acts as a more effective salt-secreting segment compared with the short proximal tubules of rainbow trout without NKCC. In the mitochondria-rich cells of the short killifish DT (5%–6% of total), we have found a more extensive basolateral membrane and better developed mitochondria compared with those present in proximal tubules. This finding suggests that a higher net rate of ion transport occurs in the DT, even though the length of the tubule is much shorter than that of the proximal tubules with the secreting type of NKCC.

Distal and collecting tubules

Rainbow trout nephrons in both SW and FW consist of a combined length of DT and CT of about 70%, and these segments possess apically located absorbing isoform of NKCC. The DT and CT are typically thought of as Na$^+$, Cl$^-$, and K$^+$ re-absorptive segments, and this model is shared within several kinds of teleost species (Hickman and Trump 1969). Nishimura et al. (1983) have measured water and ion transport in isolated nephron tubules of rainbow trout, and their results suggest that the DT from FW-adapted trout acts as a diluting segment, which is equivalent to the early distal segment of the frog kidney and the mammalian TALH (Burg and Green 1973; Rocha and Pang 1973). In tilapia, Miyazaki et al. (2002) have revealed that the kidney-specific chloride channel, OmClC-K, is specifically located in the DT, and that renal expression of mRNA of this transporter is increased in FW compared with SW. Their immunohistochemistry has also shown a basolaterally-located ClC-K transporter protein only in the DT, demonstrating

separation of transporter expression in different segments of the FW tilapia kidney and suggesting that these possibly reflect specific functional differences.

In the present study, the apically-located NKCC in the DT of killifish and trout probably plays a role in Na^+, K^+, and $2Cl^-$ absorption, and the ions will be transported back into the body through basolateral-specific ion channels such as OmClC-K, K^+ channels, and/or ion transport proteins such as the Na^+/K^+-ATPase. Killifish also have weak NKCC expression in the basolateral membrane, suggesting the differential regulation of transport in DT such that either absorption (via apical NKCC) or secretion (via basolateral NKCC) occurs. This transport model remains to be demonstrated physiologically because of the inherent complexities of examining trout kidney. However, it would represent an interesting renal regulatory system, whereby a tubule could switch between secretion and absorption, depending on the osmoregulatory needs of the animal.

Gill ion transporter distribution and its connection with kidney function

We found significant differences in the branchial distribution of NKCC both between species and between the different water environments to which they were acclimatized. Branchial mitochondria-rich cells have been studied in several species of fishes, and their physiological and morphological features have been reported (Evans et al. 2005). A previous report by Katoh et al. (2001) has shown that branchial mitochondria-rich cells of FW-acclimated killifish are morphologically much better developed than in SW and physiologically as active (Na^+/K^+-ATPase activity) as SW-type cells. The present observation, viz., that apically located NKCC is found in FW-acclimated killifish, and the previous reports suggest that FW-adapted killifish develop absorbing mitochondria-rich cells to compensate for the continuous salt secretion via the basolateral NKCC in the kidney.

In contrast, rainbow trout gill NKCC has been localized in the basolateral membrane of mitochondria-rich cells in both SW and FW. A recent study has classified mitochondria-rich cells in Mozambique tilapia embryos according to the immunolocalization of NKCC, the cystic fibrosis transmembrane conductance regulator (CFTR) Cl^- channel, and Na^+/K^+-ATPase (Hiroi et al. 2005a); Hiroi et al. (2005a) have deduced that the Na^+/K^+-ATPase-positive cell type is an immature cell (called type I), that the Na^+/K^+-ATPase-, NKCC-, and CFTR-positive cell type is an SW type (type IV), and that the Na^+/K^+-ATPase- and NKCC-positive cell is a proto- or dormant-type of the SW type cell (type III). However, NKCC-positive and Na^+/K^+-ATPase-negative cells, found in the present study, have not been found in their tilapia embryos. In our study, the Na^+/K^+-ATPase- and NKCC-positive cell cannot be concluded to be a type III or a type IV because we have not studied CFTR immunocytochemistry; however, the Na^+/K^+-ATPase- and NKCC-positive cells in SW trout might be type III or IV cells, involved in salt secretion. In terms of Na^+/K^+ ATPase and basolateral NKCC-positive cells in FW, Hiroi and McCormick (2007) have also found basolaterally localized Na^+/K^+-ATPase and NKCC in branchial mitochondria-rich cells of three salmonid species and have discussed the functional consequence of an NKCC in FW salmonids; they have hypothesized that the NKCC may provide a minimal level of salt secretory capacity, that the basolateral NKCC may function in ion uptake associated with volume regulation increase, or that the NKCC may be involved in ammonia excretion or acid/base regulation, as has been hypothesized by Wilson et al. (2000b) for the mudskipper. If the branchial NKCC in FW trout is involved in salt secretion, rather than absorption, different salt absorption mechanisms might be present in rainbow trout gills, such as the apical Na^+ channel coupled with vacuolar type H^+-ATPase, as suggested previously (Wilson et al. 2000a; Parks et al. 2007).

Because ion transport organs in an animal coordinate with each other in order to maintain blood ion concentrations within physiological levels, our findings suggest that transporter variation at the kidneys may be related to previously reported functional variation in the gill mitochondria-rich cells among fishes. According to the NKCC distribution in this study, killifish kidney, but not rainbow trout kidney, has the consistent capability to secrete salt through PII, whereas both species re-absorb NaCl through DT/CT. This is the first study to report the differential localization of NKCC protein in the PII segments of these two species. Our findings suggest that significant differences occur in the function of the proximal tubules within euryhaline fishes.

References

Beyenbach KW (1995) Secretory electrolyte transport in renal proximal tubules of fish. In: Wood CM, Shuttleworth TJ (eds) Cellular and molecular approaches to fish ionic regulation. Academic Press, San Diego, pp 85–105

Beyenbach KW, Frömter E (1985) Electrophysiological evidence for Cl secretion in shark renal proximal tubules. Am J Physiol 248: F282–F295

Beyenbach KW, Liu PLF (1996) Mechanism of fluid secretion common to aglomerular kidneys. Kidney Int 49:1543–1548

Beyenbach KW, Petzel DH, Cliff WH (1986) Renal proximal tubule of flounder. I. Physiological properties. Am J Physiol 250:R608–R615

Biemesderfer D, Payne JA, Lytle CY, Forbush B III (1996) Immunocytochemical studies of the Na-K-Cl cotransporter of shark kidney. Am J Physiol 270:F927–F936

Braun EJ, Dantzler WH (1997) Vertebrate renal system. In: Dantzler WH (ed) Handbook of physiology, section 13. Comparative physiology, vol I. Oxford University Press, New York, pp 481–576

Burg MB, Green N (1973) Function of the thick ascending limb of Henle's loop. Am J Physiol 244:F247–F254

Cliff WH, Beyenbach KW (1988) Fluid secretion in glomerular renal proximal tubules of fresh-water adapted fish. Am J Physiol 254: R154–R158

Cliff WH, Beyenbach KW (1992) Secretory renal proximal tubules in seawater- and freshwater-adapted killifish. Am J Physiol 262: F108–F116

Culter CP, Cramb G (2002) Two isoforms of the Na$^+$/K$^+$/2Cl$^-$ cotransporter are expressed in the European eel. Biochim Biophys Acta 1566:92–103

Dantzler WH (2003) Regulation of renal proximal and distal tubule transport: sodium, chloride and organic anions. Comp Biochem Physiol A136:453–478

Edwards JG, Schnitter C (1933) The renal unit in the kidney of vertebrates. Am J Anat 53:55–88

Evans DH (1979) Ion exchange mechanisms in fish gills. In: Mallory GM (ed) Comparative physiology of osmoregulation in animals, vol 1. Academic Press, San Diego, pp 305–390

Evans DH, Piermarini PM, Choe KP (2005) The multifunctional fish gill: dominant site of gas exchange, osmoregulation, acid-base regulation, and excretion of nitrogen waste. Physiol Rev 85: 97–177

Gagnon E, Forbush B, Flemmer AW, Gimenez I, Caron L, Isenring AP (2002) Functional and molecular characterization of the shark renal Na-K-Cl cotransporter: novel aspects. Am J Physiol 283: F1046–F1055

Grafflin AL (1937) Observations upon the structure of the nephron in the common eel. Am J Anat 61:21–62

Haas M (1989) Properties and diversity of (Na-K-Cl) cotransporters. Annu Rev Physiol 51:443–457

Haas M, Forbush B III (2000) The Na-K-Cl cotransporter of secretory epithelia. Annu Rev Physiol 62:515–534

Hendricks JD (1983) Urinary system. In: Yasutake WT, Wales JH (eds) Microscopic anatomy of salmonids: an atlas. Fish and Wildlife Service, US Department of the Interior, Washington, DC, pp 161–189

Hickman Jr CP, Trump BF (1969) The kidney. In: Hoar WS, Randall DJ (eds) Fish physiology, vol 1. Academic Press, New York London, pp 91–239

Hiroi J, McCormick SD (2007) Variation in salinity tolerance, gill Na$^+$/K$^+$-ATPase, Na$^+$/K$^+$/2Cl$^-$ cotransporter and mitochondria-rich cell distribution in three salmonids Salvelinus namaycush, Salvelinus fontinalis and Salmo salar. J Exp Biol 210:1015–1024

Hiroi J, McCormick SD, Ohtani-Kaneko R, Kaneko T (2005a) Functional classification of mitochondria-rich cells in euryhaline Mozambique tilapia (Oreochromis mossambicus) embryos, by means of triple immunofluorescence staining for Na$^+$/K$^+$/2Cl$^-$ cotransporter and CFTR channel. J Exp Biol 208:2023–2036

Hiroi J, Miyazaki H, Katoh F, Ohtani-Kaneko R, Kaneko T (2005b) Chloride turnover and ion transporting activities of yolk-sac preparations (yolk balls) separated from Mozambique tilapia embryos and incubated in freshwater and seawater. J Exp Biol 208:3851–3658

Igarashi P, Vanden Heuvel GB, Payne JA, Forbush B III (1995) Cloning, embryonic expression, and alternative splicing of a murine kidney-specific Na-K-Cl cotransporter. Am J Physiol 269:F405–F418

Kaplan MR, Plotkin MD, Lee WS, Xu ZC, Lytton J, Herbert SC (1996) Apical localization of the Na-K-Cl cotransporter, rBSC1, on rat thick ascending limbs. Kidney Int 49:40–47

Katoh F, Shimizu A, Uchida K, Kaneko T (2000) Shift of chloride cell distribution during early life stages in seawater-adapted killifish, Fundulus heteroclitus. Zool Sci 17:11–18

Katoh F, Hasegawa S, Kita J, Takagi Y, Kaneko T (2001) Distinct seawater and freshwater types of chloride cells in killifish, Fundulus heteroclitus. Can J Zool 79:822–829

Katoh F, Tresguerres M, Lee KM, Kaneko T, Aida K, Goss GG (2006) Cloning of rainbow trout SLC26A1: involvement in renal sulfate secretion. Am J Physiol 290:R1468–R1478

Lorin-Nebel C, Boulo V, Bodinier C, Charmantier G (2006) The Na$^+$/K$^+$/2Cl$^-$ cotransporter in the sea bass Dicentrarchus labrax during ontogeny: involvement in osmoregulation. J Exp Biol 209:4908–4922

Lytle CY, Xu JC, Biemesderfer D, Haas M, Forbush B III (1992) The Na-K-Cl cotransport protein of shark rectal gland. 1. Development of monoclonal antibodies, immunoaffinity purification, and partial biochemical characterization. J Biol Chem 267:25428–25437

Lytle CY, Xu JC, Biemesderfer D, Forbush B III (1995) Distribution and diversity of Na-K-Cl cotransport proteins: a study with monoclonal antibodies. Am J Physiol 269:C1496–C1505

Mandal AK, Wenzl JE (1979) Electron microscopy of normal kidney. In: Mandal AK (ed) Electron microscopy of the kidney. Plemium Medical Books, New York, pp 59–90

Marshall WS, Grosell M (2006) Ion transport, osmoregulation, and acid-base balance. In: Evans D, Claiborne JB (eds) The physiology of fishes, 3rd edn. CRC Press, New York, pp 179–230

Marshall WS, Lynch EM, Cozzi RRF (2002) Redistribution of immunofluoresence of CFTR anion channel and NKCC cotransporter in chloride cells during adaptation of the killifish Fundulus heteroclitus to sea water. J Exp Biol 205:1265–1273

McCormick SD, Sundell L, Bjornsson BT, Brown CL, Hiroi J (2003) Influence of salinity on the localization of Na$^+$/K$^+$-ATPase, Na$^+$/K$^+$/2Cl$^-$ cotransporter (NKCC) and CFTR channel in chloride cells of the Hawaiian goby (Stenogobius hawaiiensis). J Exp Biol 206:4575–4583

Miyazaki H, Kaneko T, Uchida S, Sasaki S, Takei Y (2002) Kidney-specific chloride channel, OmClC-K, predominantly expressed in the diluting segment of freshwater-adapted tilapia kidney. Proc Natl Acad Sci USA 99:15782–15787

Nishimura H, Imai M (1982) Control of renal function in freshwater and marine teleosts. Teleosts Fed Proc 41:2355–2360

Nishimura H, Imai M, Ogawa M (1983) Sodium chloride and water transport in the renal distal tubule of the rainbow trout. Am J Physiol 244:F247–F254

Olivereau M, Olivereau J (1977) Effect of transfer to sea water and back to fresh water on the histological structure of the eel kidney. J Comp Physiol 115:223–239

Payne JA, Forbush B III (1994) Alternatively spliced isoforms of the putative renal Na-K-Cl cotransporter are differentially distributed within the rabbit kidney. Proc Natl Acad Sci USA 91:4544–4548

Parks SK, Tresguerres M, Goss GG (2007) Cellular imaging of isolated MR cells from rainbow trout—a model for transepithelial Na$^+$ transport. Am J Physiol 292:C935–C944

Pelis RM, Zydlewski J, McCormick SD (2001) Gill Na$^+$-K$^+$-2Cl$^-$ cotransporter abundance and localization in Atlantic salmon effects of seawater and smolting. Am J Physiol 280:R1844–R1852

Praetorius HA, Spring KR (2005) A physiological view of the primary cilium. Annu Rev Physiol 67:515–529

Rocha AS, Pang PKT (1973) Sodium chloride and water transport in the medullary thick ascending limb of Henle. J Clin Invest 52:612–623

Romer AS, Parsons TS (1977) The vertebrate body, 5th edn. Saunders, Philadelphia

Scott GR, Richards JG, Forbush B, Isenring P, Schulte PM (2004) Changes in gene expression in gills of the euryhaline killifish *Fundulus heteroclitus* after abrupt salinity transfer. Am J Physiol 287:C300–C309

Tipsmark CK, Madsen SS, Seidelin M, Christensen AS, Cutler CP, Cramb G (2002) Dynamics of Na$^+$, K$^+$, 2Cl$^-$ cotransporter and Na$^+$, K$^+$-ATPase expression in the branchial epithelium of brown trout (*Salmo trutta*) and Atlantic salmon (*Salmo salar*). J Exp Zool 293:106–118

Ura K, Soyano K, Omoto N, Adachi S, Yamauchi K (1996) Localization of Na$^+$, K$^+$-ATPase in tissues of rabbit and teleosts using an antiserum detected against a partial sequence of the α-subunit. Zool Sci 13:219–227

Wilson JM, Laurent P, Tufts B, Benos DJ, Donowitz M, Vogl AW, Randall DJ (2000a) NaCl uptake by the branchial epithelium in freshwater teleost fish: an immunological approach to ion-transport protein localization. J Exp Biol 203:2279–2296

Wilson JM, Randall DJ, Donowitz M, Vogl AW, Ip AK (2000b) Immunolocalization of ion-transport proteins to branchial epithelium mitohondria-rich cells in the mudskipper (*Periophthalmodon schlosseri*). J Exp Biol 203:2297–2310

Wu YC, Lin LY, Lee TH (2003) Na$^+$, K$^+$, 2Cl$^-$ cotransporter: a novel marker for identifying freshwater- and seawater-type mitochondria-rich cells in gills of euryhaline tilapia, *Oreochromis mossambicus*. Zool Stud 42:186–192

Xu JC, Lytle C, Zhu TT, Payne JA, Benz E Jr, Forbush B III (1994) Molecular cloning and functional expression of the bumetanide-sensitive Na-K-Cl cotransporter. Proc Natl Acad Sci USA 91:2201–2205

Yokote M, Oguri M, Takeshima F (1995) Kidney. In: Hibiya T (ed) An atlas of fish histology—normal and pathological features. Fischer, New York, pp 94–133

Zhang LL, Delpire E, Vardi N (2007) NKCC1 does not accumulate chloride in developing retinal neurons. J Neurophysiol 98:266–277